Nanoscale

Cite this: *Nanoscale*, 2011, **3**, 4929

www.rsc.org/nanoscale

FEATURE ARTICLE

3D-patterned polymer brush surfaces

Xuechang Zhou,[ab] Xuqing Liu,[ab] Zhuang Xie[ab] and Zijian Zheng*[ab]

Received 3rd September 2011, Accepted 4th October 2011
DOI: 10.1039/c1nr11238d

Polymer brush-based three-dimensional (3D) structures are emerging as a powerful platform to engineer a surface by providing abundant spatially distributed chemical and physical properties. In this feature article, we aim to give a summary of the recent progress on the fabrication of 3D structures with polymer brushes, with a particular focus on the micro- and nanoscale. We start with a brief introduction on polymer brushes and the challenges to prepare their 3D structures. Then, we highlight the recent advances of the fabrication approaches on the basis of traditional polymerization time and grafting density strategies, and a recently developed feature density strategy. Finally, we provide some perspective outlooks on the future directions of engineering the 3D structures with polymer brushes.

1. Introduction

Polymer brushes,[1] polymers tethering one end on a surface, are promising materials for tailoring the surface functionality and morphology towards a wide variety of applications including responsive control of mass transport,[2–5] surface wettability tuning,[6] sensors[7,8] and actuators,[9,10] nanoparticles assembly,[11] metal coating,[12–16] and studying cell adhesion and protein adsorption.[17–21] Different from physically adhered bulk polymer thin films fabricated by solution casting methods, surface-tethered polymer brushes have much stronger interactions between the polymer chain end and the surface. As a result, polymer brushes show remarkable stability to the environment, which is critical to many applications. In general, polymer brushes can be synthesized *via* two strategies, namely "*grafting to*" and "*grafting from*".[22,23] In the "*grafting to*" strategy (Scheme 1A), polymer brushes are formed by the direct attachment of pre-made, end-functionalized polymer chains onto a surface with proper modification. Although this method is straightforward, it is not suitable for making dense and thick polymer brushes because of the steric repulsion of polymer chains and the lower attaching

[a]*Nanotechnology Center, Institute of Textiles and Clothing, The Hong Kong Polytechnic University, Hong Kong SAR, China. E-mail: tczzheng@inet.polyu.edu.hk; Fax: +852-27731432*
[b]*Advanced Research Centre for Fashion and Textiles, The Hong Kong Polytechnic University, Shenzhen Research Institute, Shenzhen, China*

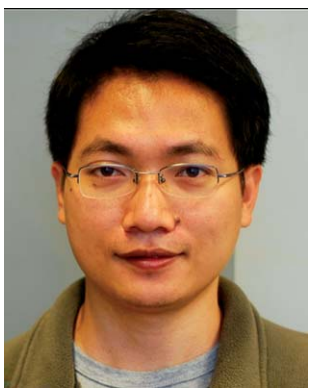

Xuechang Zhou

Dr Xuechang Zhou received his BS in polymer chemistry at the University of Science and Technology of China in 2005, and Mphil and PhD degrees in chemistry at the Chinese University of Hong Kong in 2007 and 2010, respectively. His graduate work involved the use of microfluidic systems for the study of protein crystallization, enzymatic assay, and polymer phase diagram. He is currently a Postdoctoral Fellow of Prof. Zijian Zheng's group at the Hong Kong Polytechnic University, working on the construction of surface architectures with polymer brushes at the micro- and nanoscale. His research interests include microfluidics, analytical chemistry, polymer science, and scanning probe nanolithography.

Xuqing Liu

Xuqing Liu received his B.S in chemistry at Lanzhou University in 2003. He worked as a research fellow in Lanzhou Institute of Chemical Physics, Chinese Academy of Science. He is currently a postgraduate student at the Nanotechnology Center of the Institute of Textiles and Clothing at the Hong Kong Polytechnic University. His works at Prof. Zijian Zheng's group include scanning probe nanolithography, preparation and application of conducting textiles.

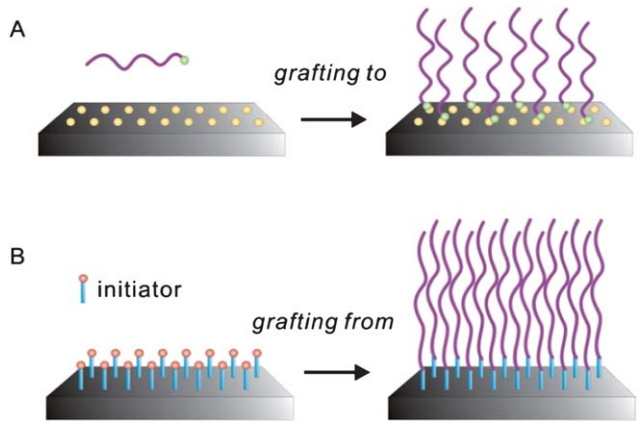

Scheme 1 Synthetic strategies of polymer brushes. (A) The "*grafting to*" approach *via* chemisorption between the end-functionalized polymer chains and the surface-immobilized complimentary groups. (B) The "*grafting from*" approach *via* SIP from initiator modified surfaces.

efficiency. On the other hand, in the "*grafting from*" strategy (Scheme 1B), polymer brushes are directly grown from an initiator-functionalized surface *via* a number of surface-initiated polymerization (SIP) methods,[24] such as surface-initiated atom transfer radial polymerization (SI-ATRP), surface-initiated reversible addition–fragmentation chain transfer (SI-RAFT) polymerization, surface-initiated nitroxide-mediated polymerization (SI-NMP), and surface-initiated photoiniferter-mediated polymerization (SI-PIMP).[23] Compared with "*grafting to*", "*grafting from*" is superior in the precise control over the polymer brush thickness, composition, and architecture, and therefore it has been widely adapted for the fabrication of the well-defined micro- and nanoarrays of polymer brushes. The fabrication process typically consists of the surface patterning of initiators in the form of one-dimensional (1D) or two-dimensional (2D) arrays by optical lithography,[25–30] soft lithography,[31,32] electron-beam lithography (EBL),[33–35] and scanning probe based lithography (SPL),[36–41] followed by bottom-up growth of polymer brushes by SIP. The progress of fabricating 1D and 2D arrays of polymer brushes has been reviewed in several articles recently.[23,42,43]

In contrast with the 1D and 2D patterns, the fabrication and engineering of well-defined 3D structures of polymer brushes are still in the early stage of development because of the remarkable complexity in simultaneous alignment of the in-plane lateral spacing and the out-of-plane height. Different from 3D polymer structures made of thin films of bulk polymer resist which can be obtained by means of serial multi-step top-down nanomachining,[44–46] the fabrication of polymer brush-based functional 3D structures requires to control not only the lateral patterning but also the molecular weight, grafting density, and composition of the polymer chains, which are extremely difficult to achieve especially when the feature size is down to the micro- and nanoscale. Macroscopic thin films of polymer brush gradients (polymer brushes with gradual thickness change) are considered to be the first demonstration of 3D structures made with polymer brushes. Indeed, not until the last five years was some significant progress made in the fabrication and application of micro- and nanostructures of 3D polymer brushes.

To date, the fabrication of 3D polymer brushes can be summarized into three strategies, namely polymerization time method, grafting density method, and a very recently developed

Zhuang Xie

Zhuang Xie received his BS in chemistry at Renmin University in 2010. Currently, he is a post-graduate student pursuing his PhD degree at the Nanotechnology Center of the Institute of Textiles and Clothing at the Hong Kong Polytechnic University. His works at Prof. Zijian Zheng's group include scanning probe nanolithography, conjugated polymers, and wearable electronics.

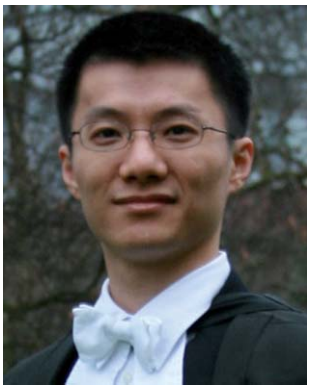

Zijian Zheng

Prof. Zijian Zheng is currently an Assistant Professor of the Institute of Textiles and Clothing at the Hong Kong Polytechnic University. His research interests include the development of surface patterning techniques, synthesis and application of graphene-based materials, structuring polymer architectures, and wearable electronic devices. Prof. Zheng received his BEng in Polymer Materials and Engineering from Department of Chemical Engineering at Tsinghua University (Beijing) in 2003. He joined Prof. Wilhelm T. S. Huck's group in 2004 and received his PhD degree in Chemistry at the University of Cambridge (UK) in 2007. His PhD thesis involved the development and application of surface patterning techniques for tailoring the surface functionalities. From January 2008 to June 2009, he worked in Prof. Chad A. Mirkin's group as a Postdoctoral Research Fellow at Northwestern University (US) focusing on the development of scanning probe nanolithography, e.g. *polymer pen lithography (PPL).*

feature density method. This feature article aims to give a focused review of this recent progress. The following sections first summarise the importance and applications of 3D structures of polymer brushes, and then focus on the highlight and discussion of the state-of-the-art techniques to fabricate micro- and nanosized 3D structures with polymer brushes. Finally, some outlooks and challenges on the future directions of 3D structures are given at the end of this article.

2. Applications of 3D structures with polymer brushes

Along with the chemistry, the 3D morphology of polymer brushes is of great importance not only for the better understanding of fundamental polymer chemistry and physics, but also for providing abundant well-defined properties for regulating many biological events.[47–51] For instance, polymer gradients with grafting-density variation were widely employed in the study of polymer physics. Genzer and co-workers carried out combinational studies of the mushroom-to-brush transition of the polymer chains by using a grafting-density gradient of polyacrylamide (PAAm).[52] Zhao *et al.* fabricated gradient-mixed poly(methyl methacrylate)/polystyrene (PMMA/PS) brushes to study the effect of relative grafting densities of two polymer chains on solvent-induced self-assembly of mixed polymer brushes.[53] What is more, polymer gradient provides a 3D template for directing the assembly of nanoparticles.[54,55] For example, Bhat *et al.* employed PAAm gradients to control the assembly of gold nanoparticles. They found that the number of particles increased as the molecular weight of polymer chains increased, and larger particles predominantly stayed near the brush–air interface, while smaller nanoparticles penetrated deeper into the polymer brushes.[54] In addition, 3D structures of polymer brushes are promising matrixes for cell studies. Washburn and co-workers fabricated poly(2-hydroxyethyl methacrylate) (PHEMA) gradients with linear variation in grafting density to regulate the cell adhesion. The cell adhesion and spreading were observed at lower grafting density, while at higher grafting density such events were hindered.[56] In another example, Gao and co-workers fabricated thermo-responsive poly(*N*-isoproylacrylamide) (PNIPAM) brushes with linear variation in film thickness to control the adhesion and detachment of biological cells.[57] The same group later fabricated RGD terminating PNIPAM–PAA gradients to regulate the cell adhesion and detachment.[58]

3. Polymerization time method

With the development of controlled/living polymerization chemistry,[23] one can tailor the chain length of polymer brushes by controlling the polymerization time. And typically, the longer the polymer chains, the thicker the polymer brushes. Therefore, 3D polymer brushes can be fabricated by changing the localized polymerization time (Scheme 2A). In the last decade, a number of strategies based on tuning the localized polymerization time have been developed to fabricate gradients of polymer brushes with linear variation in thickness. Matsuda and co-workers used a movable sample stage to create a UV exposure time gradient from photoiniferter-modified silicon substrates. In their method, a photoreactive copolymer-coated PET film was fixed on an X–Y step motor-controlled stage and was covered with a stripe patterned photomask. The film was then exposed to UV irradiation in the presence of a monomer solution. Polymer gradients with a stripe width of 500 μm were fabricated under the continuous sample movement.[59] Similarly, Harris *et al.* used a movable photomask to create polymer gradients.[60,61] On the other hand, polymerization time can be controlled by continuously removing the polymerization solution (with a μ-pump) from the chamber containing a vertically placed, initiator-coated substrate. With this so-called "draining" method, PMMA,[62] PAAm,[54] and PHEMA-*b*-PMMA[63] gradients were fabricated by Genzer and co-workers. By using a microfluidic method, Beers and co-workers prepared poly(2-(*N*,*N*′-dimethylamino)

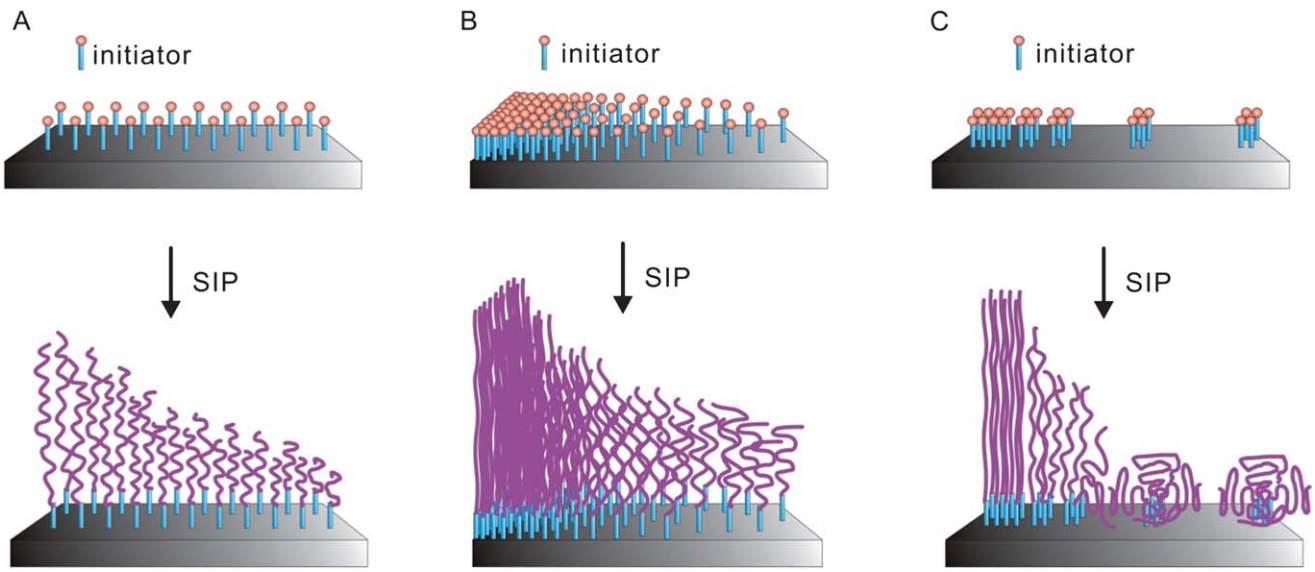

Scheme 2 Illustrations of the fabrication of 3D gradients of polymer brushes by different fabrication strategies. (A) Polymerization time method. (B) Grafting density method. (C) Feature density method.

ethylmethacrylate)-*b*-poly(*n*-butylmethacrylate) (PDMAEMA-*b*-PBMA) block copolymer brush gradients, which consist of a uniform PBMA bottom block and a molecular weight gradient of PDMAEMA top block by gradually filling the chamber containing a living PBMA brush coated substrate with the second ATRP solution.[64,65]

However, most of these examples were demonstrated at macroscopic scales. It still remains a challenge when the length scales are down to micro- and nanometre levels. Mirkin's group demonstrated an approach based on dip-pen nanolithography (DPN) and ring-opening metathesis polymerization (ROMP) to fabricate polymer arrays at the nanoscales.[37] In their method, an atomic force microscope (AFM) tip was used to deliver monomers onto the substrate at the tip–substrate contact areas and the polymerization time was controlled by the tip–substrate contact time. The height of the polymer brushes increased as a function of the tip–substrate contact time (Fig. 1). Interestingly, they found much faster polymerization kinetics compared to that in the bulk condition, which was attributed to the higher local concentration of the monomer accessible to the catalyst-activated sites on the patterned substrate.

Despite the specific example by DPN, the polymerization time method produces simple and low resolution 3D structures and is not suitable for small size patterns or arbitrary structures, which may be due to the difficulty in controlling polymerization time at small scales. To address this challenge, a popular "grafting density" method and a more recently invented "feature density" method were developed for fabricating micro- and nano-sized 3D polymer brush structures, which will be discussed in detail in the following sections.

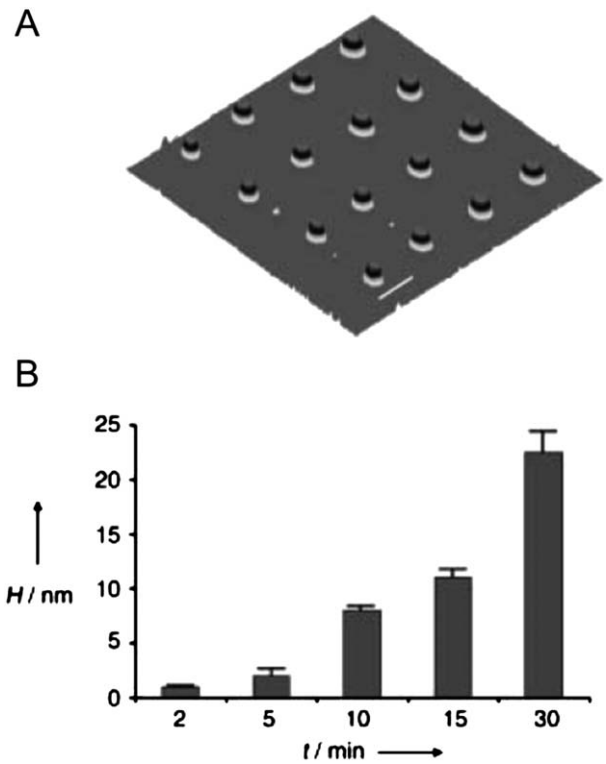

Fig. 1 Polymer structures with height variations fabricated at different polymerization time by dip-pen nanolithography (DPN) and SI-ROMP. (A) 3D topographic AFM view of an array of polymer brush dots (the scale bar is 2 μm). (B) A plot of nanostructure height (poly-exo-5-norbornen-2-ol) as a function of tip-induced polymerization time. [Adapted with permission from ref. 37, Copyright 2003 Wiley-VCH Verlag GmbH & Co. KGaA.]

4. Grafting density method

The grafting density method is by far the most widely adopted strategy for fabricating polymer brush 3D structures. Grafting density (σ) is the number of polymer chains grafted per unit area of the surface. It plays an important role in determining the chain configuration of polymer brushes.[1,52] In a good solvent, polymer brushes undergo a mushroom-to-brush configuration transition as grafting density increases. At lower grafting density, polymer chains try to maximize the contact with solvent molecules while keeping themselves stretched to a minimum, which is similar to that of free polymer chains in a solution. Such chain conformation is the so-called mushroom and has a scaling relationship $H \approx N\sigma^0$, where H and N are the thickness of brushes and degree of polymerization, respectively. As the grafting density increases, polymer chains get closer and they try to avoid chain overlapping. This results in the stretching of the chains away from the grafted surface, forming a so-called brush conformation. Such a brush conformation has a scaling relationship $H \approx N\sigma^{1/3}$. In a poor solvent or dry state, polymer chains will collapse in order to minimize the contact with solvent molecules. As a result, polymer brushes with similar chain length (*i.e.*, molecular weight) grown from low initiator grafting density areas will have more space to collapse to form shorter structures, while those grown from the high grafting density areas have less space for the collapsing so that they form taller structures.[66] Therefore, controlling the grafting density is an ideal approach to fabricate polymer brushes with variation in height both in the good solvent and poor solvent (such as dry state). For instance, thin films of polymer gradients were fabricated by SIP from substrates covered with a concentration gradient of surface initiators. Genzer *et al.*[52] fabricated a PAAm brush gradient from an initiator gradient generated by diffusion controlled vapour deposition.[67] Bohn *et al.* employed an electrochemical potential gradient to selectively desorb hexadecanethiol molecules from a gold substrate. Backfilling the exposed areas with an ATRP initiator yielded an initiator gradient, from which PNIPAM brushes were grown to a polymer gradient.[68] During the last few years, well-defined micro- and nano-sized 3D structures of polymer brushes based on the grafting density method have been demonstrated with the aid of lithographic tools such as UV interference lithography, microcontact printing (μCP), EBL, and SPL. The characteristic feature is to site selectively program the surface concentration of the initiator by these lithographic techniques, from which 3D structures of polymer brushes with height variation are formed *via* single step SIP (Scheme 2B).

4.1 UV interference lithography

Interference lithography is an optical method for fabricating periodic and quasi-periodic patterns over large areas. It is a simple process where two coherent beams interfere to produce a standing wave, which can be recorded in a photosensitive resist to yield periodic structures with a sub-100 nm resolution.

Recently, Rühe's group demonstrated the fabrication of patterned polymer brush gradients with nanometre resolution by a combination of UV interference lithography and SIP (Fig. 2).[69] This method involved the fabrication of photoinitiator patterns by UV interference patterning and subsequent growth of polymer brushes from the "surviving" initiators. The UV interference patterns were generated by using a standard so-called Lloyd setup (Fig. 2A). Briefly, a parallel beam of light that illuminated the surface was partly reflected by a mirror positioned at a 90 degree angle relative to the surface, which led to an interference pattern with strong fluctuations of the intensity of light irradiation. The extent of decomposition of the photoinitiators was controlled by different light intensities, the higher the irradiation intensity, the more the photoinitiators being decomposed. As a result, initiator patterns of the surface concentration gradient with shapes similar to the UV interference patterns were obtained (Fig. 2B), from which polymer brushes with thickness fluctuations at the nanometre scale were synthesized *via* SIP (Fig. 2C). The shapes of the polymer gradient could be tuned by adjusting the interference pattern. First of all, polymer brushes with different gradient sizes were fabricated by varying the angle of the interference light beam. PMMA brushes of varying gradient sizes were fabricated at peak-to-valley values of 155 nm, 700 nm, and 1500 nm, respectively (Fig. 2D–F). In addition, crossed gradient structures of polymer brushes could be fabricated by employing sequential multi-step UV interference patterning of the initiators (Fig. 2G–I). This method demonstrated a highly parallel way to fabricate patterned repeating polymer-brush gradients at large areas with a sub-100 nm resolution. However, this method lacks the flexibility in tuning the 3D structures into different shapes. Furthermore, it requires sophisticated optical systems for precise positioning and alignment.

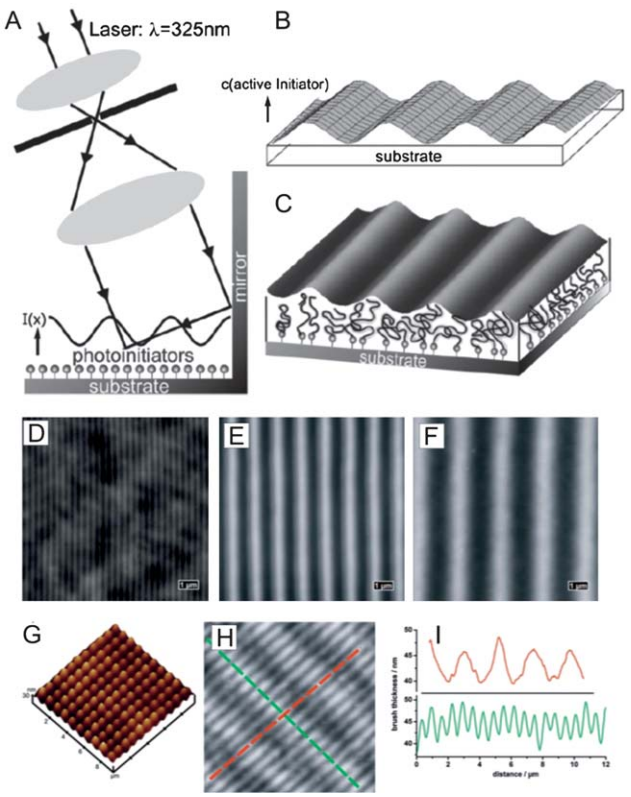

Fig. 2 3D polymer brushes with nanometre-scale gradients fabricated by a combination of UV interference and surface-initiated photo-polymerization. (A) Schematic illustration of the UV interference lithography setup. (B) Scheme of the concentration gradient of active initiators after interference lithography. (C) Overlay of an AFM image of the patterned brush with an artist's view of the brush structure. (D–F) AFM images of PMMA brushes with varying gradient sizes. (G and H) PMMA brushes with crossed gradient structures. (I) Cross-sectional profile in (H). [Adapted with permission from ref. 69, Copyright 2009 Wiley-VCH Verlag GmbH & Co. KGaA.]

4.2 μCP

μCP,[70] invented by the Whitesides group, is a simple, low-cost, and highly parallel micro- and nanofabrication tool.[31,32] It has been widely used as a bench-top method to fabricate 1D and 2D arrays of polymer brushes. Typically, it utilizes a soft polydimethyl siloxane (PDMS) stamp with relief features to directly transfer initiator inks (*e.g.* initiator terminating thiols) onto substrates (*e.g.* Au) at the areas of contact. These patterned initiators serve as templates for site-selective SIP. To fabricate 3D structures, two strategies based on μCP have been reported to date.

The Huck group developed multi-step microcontact printing (M-μCP) and subsequent SI-ATRP to fabricate polymer brushes with stepwise increment of height on gold substrates.[71,72] The key step of M-μCP is to fabricate spatially distributed surface initiator patterns containing different grafting densities (Fig. 3A). This was

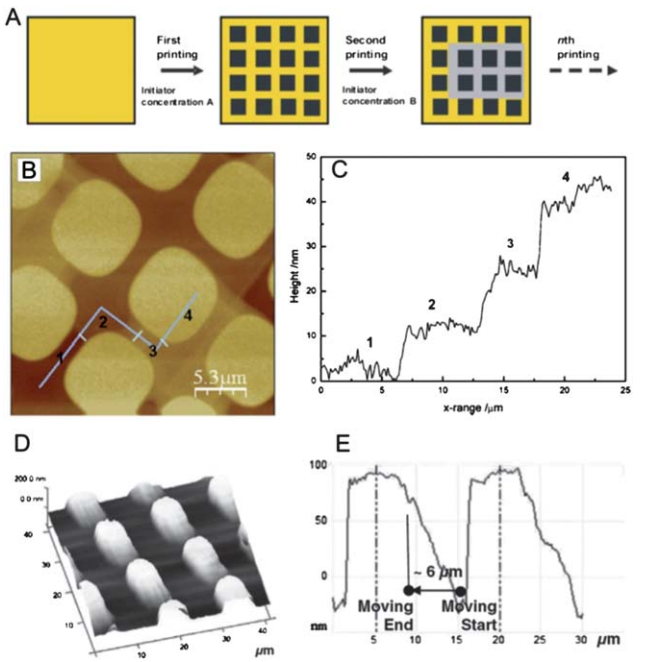

Fig. 3 3D polymer brushes fabricated by μCP. (A) Schematic illustration of a typical M-μCP process. (B–C) Polymer brushes with stepwise increment in thickness were obtained by M-μCP with inks of different ratios of initiator-terminated thiols and non-reactive alkyl thiols, and the followed up SI-ATRP. [Adapted with permission from ref. 72, Copyright 2009 Wiley-VCH Verlag GmbH & Co. KGaA.] (D–E) Polymer brush gradients fabricated by using dynamic μCP and SI-ATRP. [Adapted with permission from ref. 73, Copyright 2011 Wiley-VCH Verlag GmbH & Co. KGaA.]

achieved by using a mixture ink containing Br-terminating thiol and an inert thiol for μCP. Sequential cycles of μCP were carried out on the same substrate with change in the ratio between the two thiols at each μCP step. Finally, the bare Au surface was backfilled with inert thiols, followed by one step SI-ATRP. As a result, polymer brushes with different thickness were fabricated from patterned areas with different initiator densities. In their work, stepwise structures of poly(glycidyl methacrylate) (PGMA) brushes were fabricated by a 3-step μCP and one SI-ATRP, where the printing order was 5×5 μm^2 patterns with 100% initiator for the first step, 10×10 μm^2 patterns with 10% initiator for the second step, and 20×20 μm^2 patterns with 1% initiator for the third step (Fig. 3B). The heights of the PGMA brushes were 10 nm, 25 nm, and 45 nm, respectively (Fig. 3C).

More recently, the Zauscher group introduced an alternative method to fabricate gradients of polymer brushes by using dynamic μCP.[73] In their approach, an initiator-inked stamp was gently placed on a gold substrate, and then moved forward with fingers for a defined distance under a constant applied force. During the moving process, the ink was transferred from the stamp to the substrate *via* both ink diffusion and contact transfer. The longer the contact time, the more the initiator transferred. As a result, an initiator gradient from the moving start point to the end point was formed. Polymer brushes with gradient in thickness were then generated from the initiator gradient *via* SI-ATRP. They demonstrated gradients of PNIPAM brushes with a continuous increase in thickness from 0 to ~100 nm by this dynamic μCP method (Fig. 3D and E).

Using μCP to fabricate 3D structures of polymer brushes is low cost, high throughput, and highly scalable. Importantly, μCP is a bench-top technique which is especially friendly to chemists and can be readily used for quick tests. However, this method suffers from low pattern resolution and flexibility, and tedious control of the printing process in a semi-serial way. Therefore, in order to engineer highly defined 3D micro- and nanostructures with polymer brushes, it is necessary to employ serial surface patterning techniques with the capability to fine control the grafting density down to the nanoscale.

4.3 EBL

Different from interference lithography and μCP, EBL is a serial writing tool to fabricate nanostructures by using a focused electron beam.[33–35] It is a promising tool to fabricate high resolution 3D structures with polymer brushes because of the ultra-high patterning resolution (<10 nm) and the feasibility in programming the localized grafting density on a surface. Several exciting EBL based methods have been developed for the fabrication of 3D polymer-brush patterns in the last few years.

Electron beam chemical lithography (EBCL),[74,75] invented by Eck and Golzhauser and co-workers, was used for programming the surface concentration of initiators for fabricating 3D structures of polymer brushes.[76–78] The basic strategy is illustrated in Fig. 4A-i. Briefly, Au substrates coated with 4′-nitro-1,1′-biphenyl-4-thiol (NBT) were exposed to different irradiation doses of an electron beam. During the irradiation process, the NBT molecules were converted into cross-linked 4′-amino-1,1′-biphenyl-4-thiol (cABT), which reacted with bromoisobutyryl bromide (BIBB) to form an initiator-coated surface. The conversion yield from NBT to cABT is a function of the irradiation dose, being higher the dose, more the conversion from NBT to cABT. Therefore, a surface density gradient of bromide initiator was fabricated by programming the irradiation. PNIPAM brushes were then grown from the initiator templates *via* SI-ATRP. They demonstrated the fabrication of complex structures of PNIPAM brushes with height variations. For example, four 1 μm wide concentric rings of PNIPAM with different heights from outer to inner (16 nm, 28 nm, 52 nm, and 70 nm) were fabricated using irradiation dose of 2.5, 5, 10, and 40 mC cm^{-2}, respectively (Fig. 4A-ii). However, this method required specific nitro terminating aromatic thiol molecules which are not commercially available. Furthermore, large irradiation doses (~40 mC cm^{-2}) are needed for the conversion from nitro to amino groups.[74,75]

To resolve the drawbacks, Zharnikov and co-workers[79,80] later developed a two-step method to achieve the amino terminating gradients. They used aliphatic dodecanethiol (DDT) to replace the aromatic thiol (Fig. 4B-i). Under electron irradiation, DDT molecules were degraded into shorter aliphatic molecules, which were then exchanged by 11-aminoundecanethiol hydrochloride (AUDT). Initiator BIBB molecules were then attached to the amino tail group of AUDT. PNIPAM brushes were grown from the initiator templates *via* SI-ATRP. Gradients of PNIPAM strips with different widths (1 μm, 5 μm, and 10 μm) were demonstrated. Continuous increases from 0 nm to 200 nm in the height of PNIPAM brushes were observed as a function of the irradiation dose (Fig. 4B-ii). The advantages of this method are the use of commercially available thiol molecules and low electron irradiation doses (~2.5 mC cm^{-2}). However, this method still requires multistep formation, structuring, and functionalization of the molecular resist, and it is only applicable to Au substrates.

To overcome the limitations of using molecular resists and specific substrates, Jordan and co-workers[81–83] employed an electron-beam induced carbon deposition (EBCD) technique.[84] The key mechanism of EBCD is that electron beam irradiation of residual hydrocarbons can yield carbonaceous materials which can template subsequent photografting of polymer brushes. Again, the deposition of the carbonaceous materials is irradiation dose dependent. Based on this method, researchers demonstrated the fabrication of a step pyramid made of PS brushes from concentric carbon squares written with different electron doses on silicon nitride (Fig. 4C). The EBCD method shows a great advantage in fabricating complex 3D structures on a variety of substrates.

The common characteristic feature of the EBL-based methods is that the surface concentration of initiator can be well controlled by adjusting the irradiation dose of the electron beam.[77,79,81] The advantages of the EBL approach are the ultra-high resolution and the capability in program control of the serial writing. On the other hand, however, the EBL method requires expensive instrumentation and the throughput is very low.

4.4 SPL

SPL, *e.g.* nanoshaving, nanografting,[36,85–87] DPN,[37,88,89] a nanopen reader and writer (NPRW),[90] dip-pen nanodisplacement lithography (DNL),[91] anodization lithography,[92] and scanning

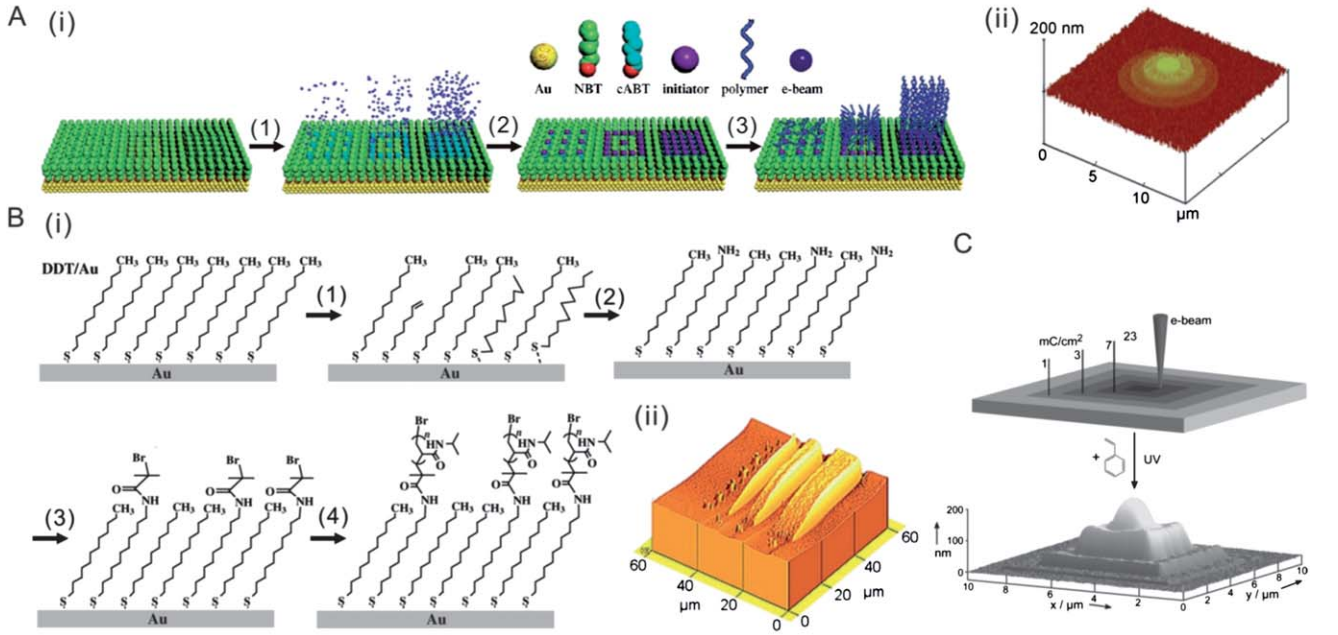

Fig. 4 EBL based methods for constructing 3D structures of polymer brushes. (A) EBCL by using an aromatic SAM resist [Adapted with permission from ref. 76, Copyright 2007 Wiley-VCH Verlag GmbH & Co. KGaA]; (B) EBCL by using an aliphatic SAM resist [Adapted with permission from ref. 79, Copyright 2008 Wiley-VCH Verlag GmbH & Co. KGaA]; and (C) EBCD for fabrication of a step pyramid shape of PS on silicon nitride substrates [Adapted with permission from ref. 81, Copyright 2009 Wiley-VCH Verlag GmbH & Co. KGaA].

near-field photolithography,[93] is a series of surface patterning techniques which utilize an ultrasharp scanning tip (or an array of tips in some examples) for the fabrication of nanostructures on surfaces. To date, only a few examples were demonstrated for making 3D structures of polymer brushes with SPL techniques.

Nanoshaving was shown to be capable of controlling the localized grafting density of initiator self-assembled monolayers (SAMs) by tuning the degree of resist removal by mechanical cleavage. For example, Zauscher *et al.* observed that longer nanoshaving time led to more removal of the self-assembled monolayers (SAMs).[36] Indeed, when the shaved substrate was backfilled with initiator molecules followed by SI-ATRP, PNIPAM brushes of different heights were fabricated on the shaved areas and the heights of PNIPAM brushes were positively related to the degree of shaving, *i.e.*, the more the shaving, the higher the brush. NPRW,[90] induced by Liu *et al.*, is a combination of the nanografting and DPN technologies, and is a promising method to engineer the nanostructures of thiol-based SAMs. Inspired by NPRW, Zheng *et al.* recently developed the DNL method which is particularly suitable for programming the nanostructures of polymer brushes.[91]

DNL is a high resolution, high registration, program controllable, solution-free, and diffusion-limited lithography tool for simultaneous destruction and construction of molecules on a surface in air and under ambient conditions at the nanometre scale. Briefly, a contact mode AFM tip inked with initiator molecules ω-mercaptoundecyl bromoisobutyrate (MUDBr) was used to shave or indent Au surfaces which had been modified with an inert SAM of 16-mercaptohexadecanoic acid (MHA). At high load (typically larger than 100 nN), MHA molecules were cleaved away by the tip, where simultaneously MUDBr molecules were transferred from the tip and assembled onto the uncovered areas of the Au surface. Finally, poly[2-(methacryloyloxy)ethyl-trimethylammonium chloride] (PMETAC) brushes were grown from the MUDBr templates *via* SI-ATRP (Fig. 5A).

Importantly, the degree of displacement is force dependent yet time independent. More MHA molecules were displaced by MUDBr at higher force, which led to thicker PMETAC brushes. A mono-increase in the thickness of PMETAC brushes from ~0 nm to ~16 nm as a consequence of an increase of tip–substrate contact force from 5 nN to 1000 nN was observed (Fig. 5B). As proof-of-concept to 3D fabrication, PMETAC brushes were grown from three concentric squared initiator templates, where the tip–substrate contact forces were 100 nN for the outer 30 μm ×30 μm square, 500 nN for the middle 11 μm ×11 μm square, and 1000 nN for the inner 1 μm ×1 μm square. Indeed, a three-layered PMETAC structure was observed by tapping mode AFM (Fig. 5C–E).

Compared with EBL based methods, scanning probe based methods do not require very expensive equipment or a vacuum environment. Therefore, it is a lower cost and more user friendly technique. However, the throughput is also low by using only one scanning tip.

5. Feature density method

In addition to the grafting density method, a new strategy namely the feature density method for constructing 3D structures of polymer brushes was reported very recently.[94] In this strategy, polymer nanobrushes, nano-sized features (nanolines or nanodots) made of polymer brushes, were used as basic building blocks to construct complex 3D structures (Scheme 2C). The

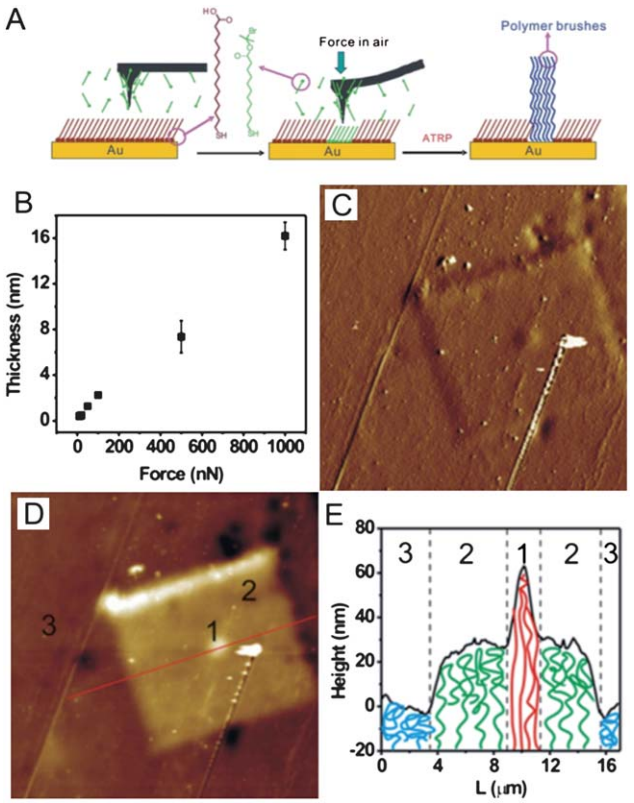

Fig. 5 3D PMETAC brushes fabricated by DNL. (A) Schematic illustration of the DNL process. (B) Force dependence graft of the height of PMETAC brushes. (C–D) AFM phase and topographic images of the as-made PMETAC brushes. (E) Cross-sectional profile of the polymer brushes indicated in (D). [Adapted with permission from ref. 91, Copyright 2010 The Royal Society of Chemistry.]

defining characteristic of the feature density method is that the rational control of the spacing between polymer nanobrushes leads to their 3D morphological evolution.

The invention of this method is based on the nanoconfinement effects of polymer nanobrushes, *i.e.*, when the feature size of polymer brushes is small enough (<500 nm), the thickness and shape of the brush are highly related to the environmental conditions as well as the feature size, apart from the chain grafting density.[95,96] It was found that the polymer chains at the edge of polymer nanobrushes spread laterally on the surface due to the combined effects of the wetting adhesion between the peripheral polymer chains and the substrate surface, and the steric repulsion from the polymer chains at the centre. Such nanoconfinement effects cause the size broadening of the polymer feature (D) compared with that of its corresponding underlining initiator feature (d), and the decrease in the thickness of the polymer nanobrush (H) compared with that of microsized features (h) synthesized under the same conditions.[77,97] The values of D/d and h/H increase (*i.e.*, the nanoconfinement effect is getting stronger) when the size of the underlining initiator decreases from 500 nm to ~20 nm. These nanoconfinement effects were reported by several groups and the studies were focused on the isolated polymer nanobrushes, *i.e.*, polymer nanobrushes separated from each other far enough without contact.

Not until recently was the interaction between spatially positioned polymer nanobrushes reported by the Zheng group (Fig. 6). In this work, arrays of nanolines or nanodots of PMETAC brushes with defined lateral spacing were fabricated by employing the DNL method and SI-ATRP.[94] At a constant tip–substrate contact force (therefore, constant grafting density), the authors observed a morphology evolution of the polymer assemblies from isolated, to bridged, and to planar structure as the spacing decreased from 1000 nm to 25 nm (Fig. 6B). In the isolated region, where the polymer nanobrushes do not contact with each other, the brush height and shape do not change and are in agreement with previous reports. As the spacing decreases, the polymer nanobrushes start to contact with the neighbouring ones and the morphology changes. The polymer chains at the edges of the nanobrushes try to stretch up because of the accumulated steric repulsion and the weakening of brush–substrate wetting, which further cause the stretching up of polymer chains at the centre of the nanobrushes. This wavy morphology was referred to as the "bridged structure". As the spacing further decreases, the amplitude of the wave decreases to approximately zero while the height of the morphology keeps increasing, this morphology being referred to as the "planar structure". Interestingly, the authors observed about 2 fold and 4 fold of increase in the height for arrays of nanolines and nanodots, respectively, which was attributed to the different extents of lateral confinement effects.

The discovery that lateral spacing can affect the 3D morphology of polymer nanobrushes is important not only to the understanding of lateral confinement of polymer nanobrushes but also to programming polymeric structures in 3D. The authors implemented this finding by introducing a feature density method

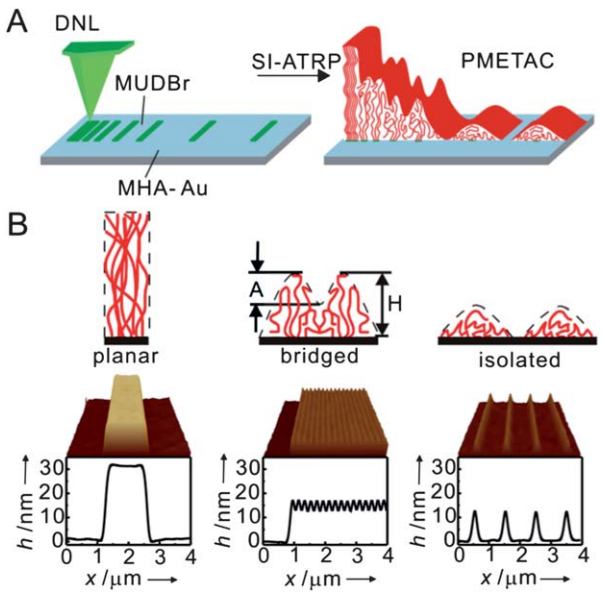

Fig. 6 Spacing dependence of PMETAC nanobrushes. (A) Schematic illustration of nanopatterning of polymer brushes *via* DNL. The morphology of polymer brushes is a function of the spacing between nanobrushes. (B) Three typical morphologies of PMETAC brushes *i.e.* planar, bridged, and isolated structures, fabricated at different spacing. [Adapted with permission from ref. 94, Copyright 2011 Wiley-VCH Verlag GmbH & Co. KGaA.]

which projects a 2D feature density array into a 3D surface morphology with polymer brushes (Fig. 7).[94]

To program the 3D structures with polymer nanobrushes, the key step is to generate arrays of nanodots with controllable spacing between the nanodots. For instance, the authors fabricated polymer gradients of different shapes including slide, conic, new moon, and pyramidal shapes (Fig. 7). A grayscale image with gradual change of brightness was first converted into a bitmap image, in which the density of white/black pixels is proportional to the brightness/darkness (Fig. 7A). Then the bitmap was used as a guide map for DNL patterning, which yielded an initiator "bitmap" comprising arrays of initiator nanodots (25 nm in diameter each) containing the density information of the white/black pixel (Fig. 7B). After SI-ATRP, PMETAC nanobrushes were grown from the as-made initiator "bitmap" (Fig. 7C). Since the lateral confinement effect at different lateral spacing leads to different height profiles, the topography of the final structure is a synergetic effect of many interactions of neighbouring nanobrushes. As a result, the topographic view of the polymer brushes represents the density information of white/black pixels from the bitmap image as well as the brightness/darkness in the greyscale image. Hence, one can fabricate arbitrary shapes of 3D structures, *e.g.*, Mona Lisa's face, by precisely designing the greyscale images (Fig. 8).

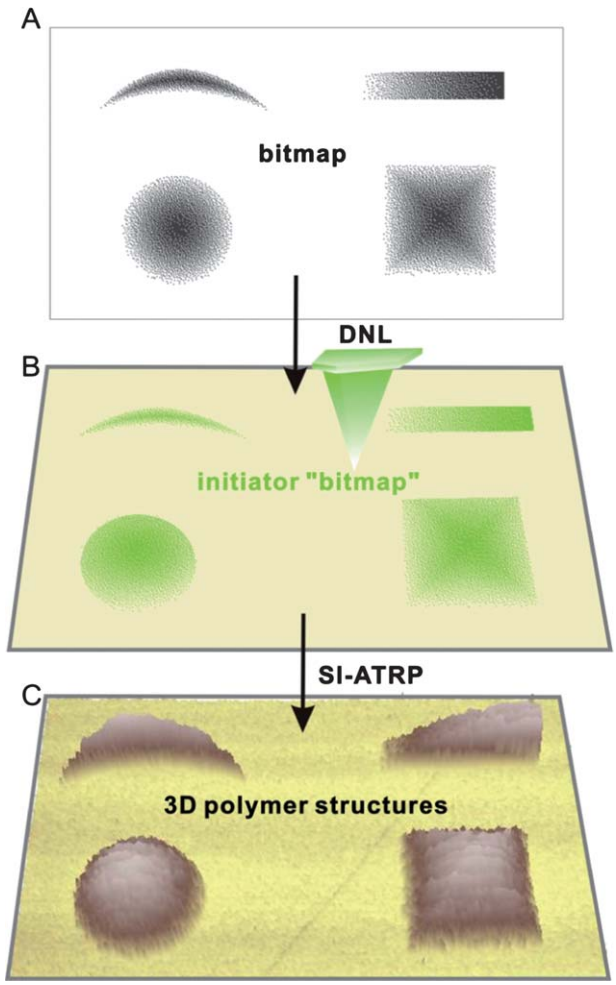

Fig. 7 Programming the 3D structures with polymer nanobrushes by the feature density method. A black-white bitmap image (A) is first transferred into an initiator "bitmap" (B) *via* the DNL, from which 3D structures of polymer nanobrushes (C), *i.e.*, slide, conic, new moon, and pyramidal shapes, are grown *via* SI-ATRP.

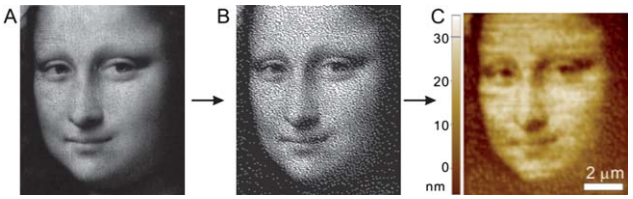

Fig. 8 3D Mona Lisa portrait fabricated by the feature density method. (A) Grayscale image of Mona Lisa's face. (B) Bitmap image converted from (A). (C) AFM topographic view of PMETAC brushes fabricated with DNL and SI-ATRP using (B) as guild map. [Adapted with permission from ref. 94, Copyright 2011 Wiley-VCH Verlag GmbH & Co. KGaA.]

Compared with the grafting density mentioned above, the feature density method is superior in its fabrication throughput and patterning feasibility.

6. Conclusions and outlook

The surface engineering and manipulating of polymer brushes offer powerful tools for the construction of functional 3D polymeric structures. Table 1 summarizes the literature on the construction of 3D structures at the micro- and nanoscale with polymer brushes, of which the fabrication methods include polymerization time, grafting density, and the feature density method. Most of the previous research focused on the use of the grafting density method, especially in EBL based methods such as EBCL and EBCD. In addition to grafting density and polymerization time, the feature density method provides a new concept to engineer complex 3D structures with polymer nanobrushes. The mechanisms of the three strategies are different. The polymerization time method relies on the control of polymer chain length. In terms of the complexity of the structures that can be made, the polymerization method is the least favourable, although it may be the simplest for making macroscopic continuous polymer gradients. Grafting density and feature density methods both actually

Table 1 Summary of methods and techniques for constructing 3D micro- and nanostructures with polymer brushes

Strategy	Lithography technique	Mechanism	Building block
Polymerization time	DPN (ref. 37)	Chain length	Single polymer chain
Grafting density	UV interference (ref. 69) μCP (ref. 71–73) EBL (ref. 76–83) SPL (ref. 36 and 91)	Chain-to-chain distance	Single polymer chain
Feature density	DNL (ref. 94)	Spacing between polymer nanobrushes	Nanostructures of polymer brushes

utilize the chain conformation evolution under different environmental conditions, where the former targets at controlling the chain-to-chain distance at the molecular level and the latter focuses on the control of feature spacing at the nanometre scale. In other words, the grafting density method uses single molecules as building blocks, while feature density uses nanofeatures as building blocks. Although both methods can produce fairly complicated 3D structures, the numbers of building blocks required (which is proportional to the number of required lithographic steps) for making the same structure by both methods are dramatically different: the feature density method can effectively reduce the number of fabrication steps. Combined with the bitmap-converting technique, the feature density method shows great potential to feasibly fabricate almost any 3D structure of polymer brushes.

Despite these successful proof-of-concept demonstrations, the fabrication and application of 3D structures of polymer brushes are still at an early stage. Future developments are required in order to address the following challenges. The first challenge is to develop strategies that allow large-scale parallel fabrication of 3D structures with nanometre resolution. One possible solution is applying highly parallel nanolithography methods such as parallel scanning near-field photolithography[93] and 2D cantilever-free scanning probe lithography, *e.g.* polymer pen lithography[98] and hard-tip soft-spring lithography.[99]

The second challenge is how to address different chemical functionalities in 3D. Post-modification of pre-fabricated 3D polymer structures is a straightforward method to selectively introduce functional groups or binding sites. Alternatively, one may use a multi-cycle fabrication strategy to introduce multiple chemical functioning groups in one 3D structure.

The third challenge is about the applications of 3D functional polymer structures. The 3D structures of polymer brushes consist of highly defined spatially resolved functions and structures. The future application developments include 3D sensing or imaging platforms for biological events; 3D bio-mimic scaffolds for biological cell study; smart systems for controlling object movement, immobilization, and distribution in 3D; program control of the folding into complex 3D structures with response to environment conditions, and so on.

Acknowledgements

Z.J.Z. acknowledges The Hong Kong Polytechnic University (Projects 1-ZV5Z, A-PK09, A-PK21) and Research Grant Council of Hong Kong (Project PolyU504111) for financial support of this work.

Notes and references

1 B. Zhao and W. J. Brittain, *Prog. Polym. Sci.*, 2000, **25**, 677–710.
2 B. Yameen, M. Ali, R. Neumann, W. Ensinger, W. Knoll and O. Azzaroni, *J. Am. Chem. Soc.*, 2009, **131**, 2070–2071.
3 B. Yameen, M. Ali, R. Neumann, W. Ensinger, W. Knoll and O. Azzaroni, *Chem. Commun.*, 2010, **46**, 1908–1910.
4 M. S. Yavuz, Y. Y. Cheng, J. Y. Chen, C. M. Cobley, Q. Zhang, M. Rycenga, J. W. Xie, C. Kim, K. H. Song, A. G. Schwartz, L. H. V. Wang and Y. N. Xia, *Nat. Mater.*, 2009, **8**, 935–939.
5 O. Azzaroni, S. E. Moya, A. A. Brown, Z. Zheng, E. Donath and W. T. S. Huck, *Adv. Funct. Mater.*, 2006, **16**, 1037–1042.
6 F. Zhou and W. T. S. Huck, *Chem. Commun.*, 2005, 5999–6001.
7 J. N. Anker, W. P. Hall, O. Lyandres, N. C. Shah, J. Zhao and R. P. Van Duyne, *Nat. Mater.*, 2008, **7**, 442–453.
8 N. Schuwer and H. A. Klok, *Adv. Mater.*, 2010, **22**, 3251–3255.
9 F. Zhou, P. M. Biesheuvel, E. Y. Chol, W. Shu, R. Poetes, U. Steiner and W. T. S. Huck, *Nano Lett.*, 2008, **8**, 725–730.
10 J. Bunsow, T. S. Kelby and W. T. S. Huck, *Acc. Chem. Res.*, 2010, **43**, 466–474.
11 R. Oren, Z. Q. Liang, J. S. Barnard, S. C. Warren, U. Wiesner and W. T. S. Huck, *J. Am. Chem. Soc.*, 2009, **131**, 1670–1671.
12 X. L. Wang, H. Hu, Y. D. Shen, X. C. Zhou and Z. J. Zheng, *Adv. Mater.*, 2011, **23**, 3090–3094.
13 X. Q. Liu, H. X. Chaing, Y. Li, W. T. S. Huck and Z. J. Zheng, *ACS Appl. Mater. Interfaces*, 2010, **2**, 529–535.
14 D. Paripovic and H. A. Klok, *ACS Appl. Mater. Interfaces*, 2011, **3**, 910–917.
15 Z. L. Liu, H. Y. Hu, B. Yu, M. A. Chen, Z. J. Zheng and F. Zhou, *Electrochem. Commun.*, 2009, **11**, 492–495.
16 O. Azzaroni, Z. J. Zheng, Z. Q. Yang and W. T. S. Huck, *Langmuir*, 2006, **22**, 6730–6733.
17 N. Ayres, *Polym. Chem.*, 2010, **1**, 769–777.
18 P. M. Mendes, *Chem. Soc. Rev.*, 2008, **37**, 2512–2529.
19 R. Barbey, E. Kauffmann, M. Ehrat and H. A. Klok, *Biomacromolecules*, 2010, **11**, 3467–3479.
20 S. Tugulu, A. Arnold, I. Sielaff, K. Johnsson and H. A. Klok, *Biomacromolecules*, 2005, **6**, 1602–1607.
21 S. Tugulu, P. Silacci, N. Stergiopulos and H. A. Klok, *Biomaterials*, 2007, **28**, 2536–2546.
22 B. Zdyrko and I. Luzinov, *Macromol. Rapid Commun.*, 2011, **32**, 859–869.
23 R. Barbey, L. Lavanant, D. Paripovic, N. Schuwer, C. Sugnaux, S. Tugulu and H. A. Klok, *Chem. Rev.*, 2009, **109**, 5437–5527.
24 S. Edmondson, V. L. Osborne and W. T. S. Huck, *Chem. Soc. Rev.*, 2004, **33**, 14–22.
25 M. Husemann, M. Morrison, D. Benoit, K. J. Frommer, C. M. Mate, W. D. Hinsberg, J. L. Hedrick and C. J. Hawker, *J. Am. Chem. Soc.*, 2000, **122**, 1844–1845.
26 O. Prucker, M. Schimmel, G. Tovar, W. Knoll and J. Ruhe, *Adv. Mater.*, 1998, **10**, 1073–1077.
27 F. Zhou, W. M. Liu, J. C. Hao, T. Xu, M. Chen and Q. J. Xue, *Adv. Funct. Mater.*, 2003, **13**, 938–942.
28 Y. Nakayama and T. Matsuda, *Macromolecules*, 1996, **29**, 8622–8630.
29 S. Tugulu, M. Harms, M. Fricke, D. Volkmer and H. A. Klok, *Angew. Chem., Int. Ed.*, 2006, **45**, 7458–7461.
30 C. Padeste, H. H. Solak, H. P. Brack, M. Slaski, S. A. Gursel and G. G. Scherer, *J. Vac. Sci. Technol., B*, 2004, **22**, 3191–3195.
31 B. D. Gates, Q. B. Xu, M. Stewart, D. Ryan, C. G. Willson and G. M. Whitesides, *Chem. Rev.*, 2005, **105**, 1171–1196.
32 F. Zhou, Z. J. Zheng, B. Yu, W. M. Liu and W. T. S. Huck, *J. Am. Chem. Soc.*, 2006, **128**, 16253–16258.
33 M. Y. Paik, Y. Y. Xu, A. Rastogi, M. Tanaka, Y. Yi and C. K. Ober, *Nano Lett.*, 2010, **10**, 3873–3879.
34 S. J. Ahn, M. Kaholek, W. K. Lee, B. LaMattina, T. H. LaBean and S. Zauscher, *Adv. Mater.*, 2004, **16**, 2141–2145.
35 A. Rastogi, M. Y. Paik, M. Tanaka and C. K. Ober, *ACS Nano*, 2010, **4**, 771–780.
36 M. Kaholek, W. K. Lee, B. LaMattina, K. C. Caster and S. Zauscher, *Nano Lett.*, 2004, **4**, 373–376.
37 X. G. Liu, S. W. Guo and C. A. Mirkin, *Angew. Chem., Int. Ed.*, 2003, **42**, 4785–4789.
38 D. S. Ginger, H. Zhang and C. A. Mirkin, *Angew. Chem., Int. Ed.*, 2004, **43**, 30–45.
39 X. Z. Zhou, F. Boey, F. W. Huo, L. Huang and H. Zhang, *Small*, 2011, **7**, 2273–2289.
40 X. Z. Zhou, Y. H. Chen, B. Li, G. Lu, F. Y. C. Boey, J. Ma and H. Zhang, *Small*, 2008, **4**, 1324–1328.
41 X. Zhou, F. Boey and H. Zhang, *Chem. Soc. Rev.*, 2011, **40**, 5221–5231.
42 R. Ducker, A. Garcia, J. M. Zhang, T. Chen and S. Zauscher, *Soft Matter*, 2008, **4**, 1774–1786.
43 Z. H. Nie and E. Kumacheva, *Nat. Mater.*, 2008, **7**, 277–290.
44 A. W. Knoll, D. Pires, O. Coulembier, P. Dubois, J. L. Hedrick, J. Frommer and U. Duerig, *Adv. Mater.*, 2010, **22**, 3361–3365.
45 D. Pires, J. L. Hedrick, A. De Silva, J. Frommer, B. Gotsmann, H. Wolf, M. Despont, U. Duerig and A. W. Knoll, *Science*, 2010, **328**, 732–735.

46 Y. D. Yan, Z. J. Hu, X. S. Zhao, T. Sun, S. Dong and X. D. Li, *Small*, 2010, **6**, 724–728.
47 R. R. Bhat, M. R. Tomlinson, T. Wu and J. Genzer, *Adv. Polym. Sci.*, 2006, **198**, 51–124.
48 S. Morgenthaler, C. Zink and N. D. Spencer, *Soft Matter*, 2008, **4**, 419–434.
49 R. Ogaki, M. Alexander and P. Kingshott, *Mater. Today*, 2010, **13**, 22–35.
50 P. Roach, T. Parker, N. Gadegaard and M. R. Alexander, *Surf. Sci. Rep.*, 2010, **65**, 145–173.
51 C. G. Simon and S. Lin-Gibson, *Adv. Mater.*, 2011, **23**, 369–387.
52 T. Wu, K. Efimenko and J. Genzer, *J. Am. Chem. Soc.*, 2002, **124**, 9394–9395.
53 B. Zhao, *Langmuir*, 2004, **20**, 11748–11755.
54 R. R. Bhat, J. Genzer, B. N. Chaney, H. W. Sugg and A. Liebmann-Vinson, *Nanotechnology*, 2003, **14**, 1145–1152.
55 I. Luzinov, S. Minko and V. V. Tsukruk, *Soft Matter*, 2008, **4**, 714–725.
56 Y. Mei, T. Wu, C. Xu, K. J. Langenbach, J. T. Elliott, B. D. Vogt, K. L. Beers, E. J. Amis and N. R. Washburn, *Langmuir*, 2005, **21**, 12309–12314.
57 L. H. Li, Y. Zhu, B. Li and C. Y. Gao, *Langmuir*, 2008, **24**, 13632–13639.
58 L. H. Li, J. D. Wu and C. Y. Gao, *Colloids Surf., B*, 2011, **85**, 12–18.
59 J. Higashi, Y. Nakayama, R. E. Marchant and T. Matsuda, *Langmuir*, 1999, **15**, 2080–2088.
60 B. P. Harris, J. K. Kutty, E. W. Fritz, C. K. Webb, K. J. L. Burg and A. T. Metters, *Langmuir*, 2006, **22**, 4467–4471.
61 B. P. Harris and A. T. Metters, *Macromolecules*, 2006, **39**, 2764–2772.
62 M. R. Tomlinson and J. Genzer, *Macromolecules*, 2003, **36**, 3449–3451.
63 M. R. Tomlinson and J. Genzer, *Chem. Commun.*, 2003, 1350–1351.
64 C. Xu, T. Wu, J. D. Batteas, C. M. Drain, K. L. Beers and M. J. Fasolka, *Appl. Surf. Sci.*, 2006, **252**, 2529–2534.
65 C. Xu, T. Wu, C. M. Drain, J. D. Batteas, M. J. Fasolka and K. L. Beers, *Macromolecules*, 2006, **39**, 3359–3364.
66 D. M. Jones, A. A. Brown and W. T. S. Huck, *Langmuir*, 2002, **18**, 1265–1269.
67 M. K. Chaudhury and G. M. Whitesides, *Science*, 1992, **256**, 1539–1541.
68 X. J. Wang, H. L. Tu, P. V. Braun and P. W. Bohn, *Langmuir*, 2006, **22**, 817–823.
69 C. Schuh, S. Santer, O. Prucker and J. Ruhe, *Adv. Mater.*, 2009, **21**, 4706–4710.
70 Y. N. Xia and G. M. Whitesides, *Angew. Chem., Int. Ed.*, 1998, **37**, 551–575.
71 T. S. Kelby, M. Wang and W. T. S. Huck, *Adv. Funct. Mater.*, 2011, **21**, 652–657.
72 M. Wang, J. E. Comrie, Y. P. Bai, X. M. He, S. Y. Guo and W. T. S. Huck, *Adv. Funct. Mater.*, 2009, **19**, 2236–2243.
73 T. Chen, R. Jordan and S. Zauscher, *Small*, 2011, **7**, 2148–2152.
74 W. Eck, V. Stadler, W. Geyer, M. Zharnikov, A. Golzhauser and M. Grunze, *Adv. Mater.*, 2000, **12**, 805–808.
75 A. Golzhauser, W. Eck, W. Geyer, V. Stadler, T. Weimann, P. Hinze and M. Grunze, *Adv. Mater.*, 2001, **13**, 803–806.
76 Q. He, A. Kueller, S. Schilp, F. Leisten, H. A. Kolb, M. Grunze and J. B. Li, *Small*, 2007, **3**, 1860–1865.
77 M. Steenackers, A. Kueller, N. Ballav, M. Zharnikov, M. Grunze and R. Jordan, *Small*, 2007, **3**, 1764–1773.
78 M. Steenackers, A. Kuller, S. Stoycheva, M. Grunze and R. Jordan, *Langmuir*, 2009, **25**, 2225–2231.
79 N. Ballav, S. Schilp and M. Zharnikov, *Angew. Chem., Int. Ed.*, 2008, **47**, 1421–1424.
80 S. Schilp, N. Ballav and M. Zharnikov, *Angew. Chem., Int. Ed.*, 2008, **47**, 6786–6789.
81 M. Steenackers, R. Jordan, A. Kuller and M. Grunze, *Adv. Mater.*, 2009, **21**, 2921–2925.
82 M. Steenackers, A. M. Gigler, N. Zhang, F. Deubel, M. Seifert, L. H. Hess, C. H. Y. X. Lim, K. P. Loh, J. A. Garrido, R. Jordan, M. Stutzmann and I. D. Sharp, *J. Am. Chem. Soc.*, 2011, **133**, 10490–10498.
83 N. A. Hutter, M. Steenackers, A. Reitinger, O. A. Williams, J. A. Garrido and R. Jordan, *Soft Matter*, 2011, **7**, 4861–4867.
84 W. F. van Dorp and C. W. Hagen, *J. Appl. Phys.*, 2008, **104**, 081310.
85 S. Xu and G. Y. Liu, *Langmuir*, 1997, **13**, 127–129.
86 S. Xu, S. Miller, P. E. Laibinis and G. Y. Liu, *Langmuir*, 1999, **15**, 7244–7251.
87 M. Barczewski, S. Walheim, T. Heiler, A. Blaszczyk, M. Mayor and T. Schimmel, *Langmuir*, 2010, **26**, 3623–3628.
88 R. D. Piner, J. Zhu, F. Xu, S. H. Hong and C. A. Mirkin, *Science*, 1999, **283**, 661–663.
89 W. K. Lee, L. J. Whitman, J. Lee, W. P. King and P. E. Sheehan, *Soft Matter*, 2008, **4**, 1844–1847.
90 N. A. Amro, S. Xu and G. Y. Liu, *Langmuir*, 2000, **16**, 3006–3009.
91 X. Q. Liu, Y. Li and Z. J. Zheng, *Nanoscale*, 2010, **2**, 2614–2618.
92 W. K. Lee, K. C. Caster, J. Kim and S. Zauscher, *Small*, 2006, **2**, 848–853.
93 E. ul Haq, Z. M. Liu, Y. A. Zhang, S. A. A. Ahmad, L. S. Wong, S. P. Armes, J. K. Hobbs, G. J. Leggett, J. Micklefield, C. J. Roberts and J. M. R. Weaver, *Nano Lett.*, 2010, **10**, 4375–4380.
94 X. C. Zhou, X. L. Wang, Y. D. Shen, Z. Xie and Z. J. Zheng, *Angew. Chem., Int. Ed.*, 2011, **50**, 6506–6510.
95 A. M. Jonas, Z. J. Hu, K. Glinel and W. T. S. Huck, *Nano Lett.*, 2008, **8**, 3819–3824.
96 A. M. Jonas, Z. J. Hu, K. Glinel and W. T. S. Huck, *Macromolecules*, 2008, **41**, 6859–6863.
97 W. K. Lee, M. Patra, P. Linse and S. Zauscher, *Small*, 2007, **3**, 63–66.
98 F. W. Huo, Z. J. Zheng, G. F. Zheng, L. R. Giam, H. Zhang and C. A. Mirkin, *Science*, 2008, **321**, 1658–1660.
99 W. Shim, A. B. Braunschweig, X. Liao, J. N. Chai, J. K. Lim, G. F. Zheng and C. A. Mirkin, *Nature*, 2011, **469**, 516–521.